AD_____

AWARD NUMBER: W81XWH-07-1-0301

TITLE: A Model System To Investigate the Effect of BRCA1 and/or p53 Inactivation in the Ovarian Stroma on Growth and Transformation Potential of the Ovarian Epithelium

PRINCIPAL INVESTIGATOR: Denise C. Connolly, Ph.D.

CONTRACTING ORGANIZATION: Fox Chase Cancer Center
Philadelphia, PA 19111

REPORT DATE: October 2009

TYPE OF REPORT: Final

PREPARED FOR: U.S. Army Medical Research and Materiel Command
Fort Detrick, Maryland 21702-5012

REPORT DOCUMENTATION PAGE

Form Approved
OMB No. 0704-0188

1. REPORT DATE	2. REPORT TYPE	3. DATES COVERED
1 October 2009	Final	1 Apr 2007 – 30 Sep 2009

4. TITLE AND SUBTITLE

A Model System To Investigate the Effect of BRCA1 and/or p53 Inactivation in the Ovarian Stroma on Growth and Transformation Potential of the Ovarian Epithelium

5a. CONTRACT NUMBER

5b. GRANT NUMBER
W81XWH-07-1-0301

5c. PROGRAM ELEMENT NUMBER

6. AUTHOR(S)

Denise C. Connolly, Ph.D.

E-Mail: Denise.Connolly@fccc.edu

5d. PROJECT NUMBER

5e. TASK NUMBER

5f. WORK UNIT NUMBER

7. PERFORMING ORGANIZATION NAME(S) AND ADDRESS(ES)

Fox Chase Cancer Center
Philadelphia, PA 19111

8. PERFORMING ORGANIZATION REPORT NUMBER

9. SPONSORING / MONITORING AGENCY NAME(S) AND ADDRESS(ES)
U.S. Army Medical Research and Materiel Command
Fort Detrick, Maryland 21702-5012

10. SPONSOR/MONITOR'S ACRONYM(S)

11. SPONSOR/MONITOR'S REPORT NUMBER(S)

12. DISTRIBUTION / AVAILABILITY STATEMENT
Approved for Public Release; Distribution Unlimited

13. SUPPLEMENTARY NOTES

14. ABSTRACT

Women carrying germline mutations in BRCA1 are at high risk for developing ovarian cancer and mutations in p53 are frequently detected in ovarian tumors. The tumor microenvironment plays an important role in cancer progression. The tumor stroma promotes angiogenesis and is a source of growth factors, chemokines, and extracellular matrix (ECM) molecules that promotes carcinoma progression. We investigated the effects of loss of function of BRCA1 or BRCA1 and Trp53 in the stroma on the growth and neoplastic transformation of epithelial cells using 2D and 3D in vitro cell culture models. A growing number of studies suggest that selective inactivation of BRCA1 or p53 in the stroma surrounding tumors plays a direct role in tumor progression. Therefore, to directly test the hypothesis that stromal cells exert cell-nonautonomous effects on ovarian epithelial cell growth and neoplastic transformation, we examined the effects of culturing mouse ovarian surface epithelial (MOSE) cells with ECM and conditioned media from stromal cells in which BRCA1 or BRCA1 and Trp53 were inactivated.

15. SUBJECT TERMS
BRCA1, p53, ovarian cancer, epithelial/stromal interaction

16. SECURITY CLASSIFICATION OF:			17. LIMITATION OF ABSTRACT	18. NUMBER OF PAGES	19a. NAME OF RESPONSIBLE PERSON
a. REPORT	b. ABSTRACT	c. THIS PAGE			19b. TELEPHONE NUMBER *(include area code)*
U	U	U	UU	13	USAMRMC

Standard Form 298 (Rev. 8-98)
Prescribed by ANSI Std. Z39.18

Table of Contents

A Model System to Investigate the effect of *BRCA1* and/or *p53* Inactivation in the Ovarian Stroma on Growth and Transformation Potential of the Ovarian Epithelium

PI: Denise C. Connolly

Final Report, October 22, 2009

Introduction:

Women carrying germline mutations in *BRCA1* are at high risk for developing epithelial ovarian cancer (EOC) [1]. A number of independent studies [2-5] have shown that *BRCA1*-associated cases of EOC also have a high frequency (ranging from 70-90%) of mutations of *p53*, suggesting that loss of functional p53 contributes to hereditary ovarian cancer. The mechanisms by which mutation or loss of *BRCA1* and *p53* contribute to ovarian tumorigenesis remain unresolved. However, several recent studies [6-9] suggest that selective inactivation of *BRCA1* or *p53* in the stroma surrounding tumors plays a direct role in tumor progression. Using a Cre/LoxP strategy to specifically inactivate *Brca1*, Chodankar et al. showed that benign epithelial neoplasms developed in the ovaries and uterine horns of mice in which *Brca1* was conditionally inactivated in granulosa cells [6]. Interestingly, Cre-mediated excision of the *Brca1* alleles was not detected within the epithelial lesions themselves, suggesting that inactivation of *Brca1* in granulosa cells is sufficient to initiate neoplastic transformation in the epithelial compartment in a cell non-autonomous manner. Other studies [8, 9] showed a higher rate of loss of heterozygosity or allelic imbalance of genes, including *p53*, in the stroma surrounding *BRCA1/2*-related tumors compared to sporadic cancers, suggesting that alterations present in tumor stroma play a direct role in tumor progression in *BRCA*-associated cancers.

It is well established that both genetic and/or epigenetic alterations within the underlying tumor stroma have a direct effect on tumor progression (reviewed in [11]). In a mouse model of prostate cancer, selective mutation of *p53* was identified in tumor-associated stroma leading to the selection of a highly proliferative *p53* null subpopulation of fibroblasts that contributed to tumor progression [7]. Moreover, a recent study showed that cells exhibiting a senescence-associated secretory phenotype (SASP) contribute to epithelial to mesenchymal transitions and invasiveness in a cell non-autonomous manner, with inactivation of *p53* being a major contributor to these pro-malignant paracrine activities [10]. Hence, it is clear that stromal-epithelial interactions are critical to both normal ovarian tissue function and to the process of epithelial tumor initiation and progression.

Based on the above observations, we hypothesized that inactivation of *BRCA1* and/or *p53* in ovarian stroma would alter the paracrine signaling environment, including the extracellular matrix (ECM), thereby contributing to preneoplastic or neoplastic changes the ovarian epithelium. For example, growth factors, chemokines and/or cytokines secreted by the surrounding stroma may regulate signal transduction pathways that mediate cell proliferation or apoptosis. Alternatively, interactions between integrins in epithelial cells and the surrounding stromal ECM may modulate outside-in signaling cascades that alter cell morphology, adhesion, invasion and/or growth.

To address this experimentally, we investigated the contribution of the stroma in mediating the growth and neoplastic transformation of mouse ovarian surface epithelial (MOSE) cells. We developed a three-dimensional (3D) *in vitro* culture system utilizing primary MOSE and stromal cells isolated from the ovaries of mice harboring LoxP flanked (floxed) alleles of *Brca1* ($Brca1^{LoxP/LoxP}$) or *Brca1* and *Trp53* ($Brca1^{LoxP/LoxP};Trp53^{LoxP/LoxP}$). Primary MOSE and stromal cells were infected with control adenovirus (*Ad5-CMV-GFP*), or adenovirus encoding Cre-recombinase, (*Ad5-CMV-Cre-GFP*). Cre-mediated excision of the floxed alleles results in cells with the following mutant genotypes: $Brca1^{\Delta 5\text{-}13}$ and $Brca1^{\Delta 5\text{-}13};Trp53^{\Delta 2\text{-}10}$. Stromal cells were grown as 3D cultures and conditioned culture medium was collected and extracellular matrices (ECMs) were derived from these cultures. Primary MOSE cells were grown within the 3D matrices or on standard cell culture plastic (2D). Cultures were also grown in the absence or presence of conditioned medium collected from the stromal cells, allowing us to examine the cell non-autonomous contributions of the stroma on

growth of ovarian surface epithelial cells.

Specific aims:

1) Determine whether paracrine/autocrine factors secreted by 3D stromal cultures with inactivation of *Brca1* and/or *Trp53* have an enhanced ability to influence the growth and transformation potential of normal and *Brca1* and/or *Trp53* mutant MOSE cells.

2) Demonstrate that 3D extracellular matrices isolated from genetically inactivated stromal cells (*e.g.*, *Brca1* inactive) facilitate growth and transformation potential of normal ovarian epithelial cells, and that genetically modified epithelial cells (*e.g.*, *Brca1* inactive) acquire a transformation advantage when cultured within primed or modified stromal ECM.

Body:

The following goals were completed: 1) isolation of MOSE and ovarian stromal cells from mice expressing conditional alleles of *Brca1* and/or *Trp53*, 2) optimization of 3D stromal culture methods, 3) characterization of FN and type I collagen expression in control ($Brca1^{LoxP/LoxP}$ and $Brca1^{LoxP/LoxP};Trp53^{LoxP/LoxP}$) and mutant ($Brca1^{\Delta 5\text{-}13}$ and $Brca1^{\Delta 5\text{-}13};Trp53^{\Delta 2\text{-}10}$) 3D stromal cultures, 4) analysis of proliferation in control and mutant stromal and MOSE cells, 5) analysis of invasion of control and mutant MOSE cells through 3D matrices isolated from control and mutant 3D ECMs, 6) characterization of apoptosis in control and mutant MOSE cells cultured in the presence of conditioned media or on 3D ECMs from control and mutant 3D stromal cells and 7) analysis of proliferation in control and mutant MOSE cells cultured on control and mutant 3D ECMs. All procedures involving animals were approved by Fox Chase Institutional Animal Care and Use Committee.

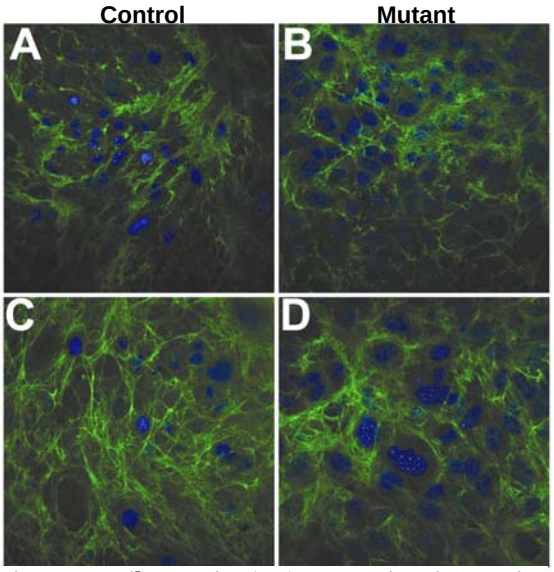

Figure 1. Fibronectin (FN) expression in ovarian stromal cells grown in 3D. A) $Brca1^{LoxP/LoxP}$, B) $Brca1^{\Delta 5\text{-}13}$, C) $Brca^{LoxP/LoxP};Trp53^{LoxP/LoxP}$ and D) $Brca1^{\Delta 5\text{-}13};Trp53^{\Delta 2\text{-}10}$ stromal cells were grown as 3-D cultures and subjected to indirect IF for FN. Z-sections of cultures imaged on a confocal microscope depict FN fibers (green) and nuclei (DAPI stained, blue).

To establish an *in vitro* model system to study epithelial-stromal cell interactions, primary cultures of MOSE and ovarian stromal cells were isolated from the ovaries of $Brca1^{LoxP/LoxP}$ and $Brca1^{LoxP/LoxP};Trp53^{LoxP/LoxP}$ mice. Cultures were infected with adenovirus expressing Cre-recombinase for excision and recombination of floxed sequences. The effects of loss of *Brca1* or *Brca1* and *Trp53* expression in MOSE and stromal cells were analyzed by evaluating proliferation and apoptosis in MOSE cells cultured on standard plastic (2D), on 3D ECM isolated from ovarian stromal cells.

We first analyzed the expression of fibronectin (FN), and type I collagen (Col I) in these cells to verify consistent stromal cell phenotype and morphology after excision of

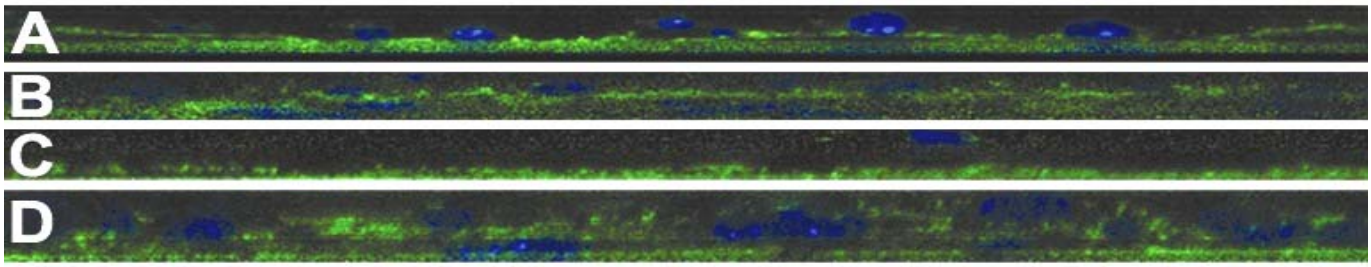

Figure 2. Orthogonal images through 3D ovarian stromal cell cultures. Z-sections from a stack of images acquired on a confocal microscope were compiled to construct orthogonal views through the XZ plane of individual 3-D stromal cultures. Each orthogonal view demonstrates the thickness of the 3-D ovarian stromal cultures with the following genotypes: (A) $Brca1^{LoxP/LoxP}$, (B) $Brca1^{\Delta 5\text{-}13}$, (C) $Brca^{LoxP/LoxP};Trp53^{LoxP/LoxP}$ and (D) $Brca1^{\Delta 5\text{-}13};Trp53^{\Delta 2\text{-}10}$. Cells are stained with FN (green) and nuclei stained with DAPI (blue).

Brca1 or *Brca1* and *Trp53*,. Stromal cells isolated from the ovaries of $Brca1^{LoxP/LoxP}$ and $Brca1^{LoxP/LoxP}$;$Trp53^{LoxP/LoxP}$ mice were grown over a period of eight days in the presence of ascorbic acid to allow cells to establish a 3D structure and secrete ECM [12]. Indirect immunofluorescent (IF) imaging of FN and Col I was performed, and confocal images through the Z axis (Z-sections) were taken. The images show that the organization of FN (Fig. 1) was similar in $Brca1^{LoxP/LoxP}$ and $Brca1^{LoxP/LoxP}$;$Trp53^{LoxP/LoxP}$ stromal cells, and stromal cells in which *Brca1* alone or *Brca1* and *Trp53* were inactivated by Cre-mediated excision of floxed sequences ($Brca1^{\Delta 5\text{-}13}$ and $Brca1^{\Delta 5\text{-}13}$;$Trp53^{\Delta 2\text{-}10}$ cells). These results suggest that loss of *Brca1* alone or in combination with *Trp53* in ovarian stromal cells does not result in the formation of parallel bundles of FN as is sometimes observed in tumor-associated fibroblasts [11]. Orthogonal views through the XZ plane of the stromal cultures (Fig. 2) were constructed from individual Z-sections and revealed that $Brca1^{\Delta 5\text{-}13}$;$Trp53^{\Delta 2\text{-}10}$ stromal cells (cells, Fig. 2D) form a thicker 3D structure in culture than $Brca1^{\Delta 5\text{-}13}$ stromal cells (Fig. 2B) or cells with intact *Brca1* or *Brca1* and *Trp53*

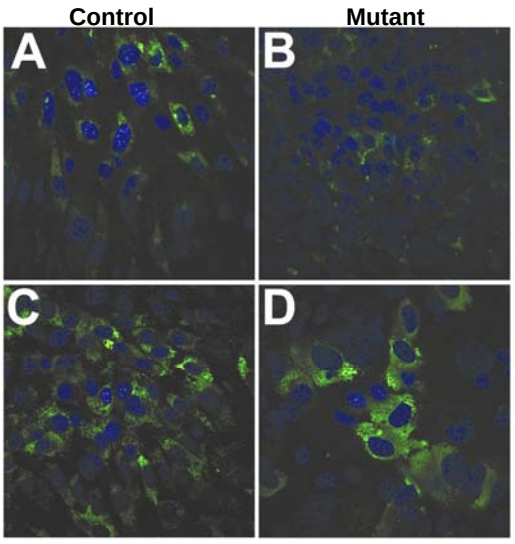

Figure 3. Type I collagen (Col I) expression in primary cultures of ovarian stromal cells grown in 3-D. A) $Brca1^{LoxP/LoxP}$, B) $Brca1^{\Delta 5\text{-}13}$, C) $Brca1^{LoxP/LoxP}$;$Trp53^{LoxP/LoxP}$ and D) $Brca1^{\Delta 5\text{-}13}$;$Trp53^{\Delta 2\text{-}10}$ stromal cells grown as 3-D cultures and subjected to indirect IF detection of Col I. Z-sections of cultures imaged on a confocal microscope depict Col I (green) and nuclei (DAPI stained, blue).

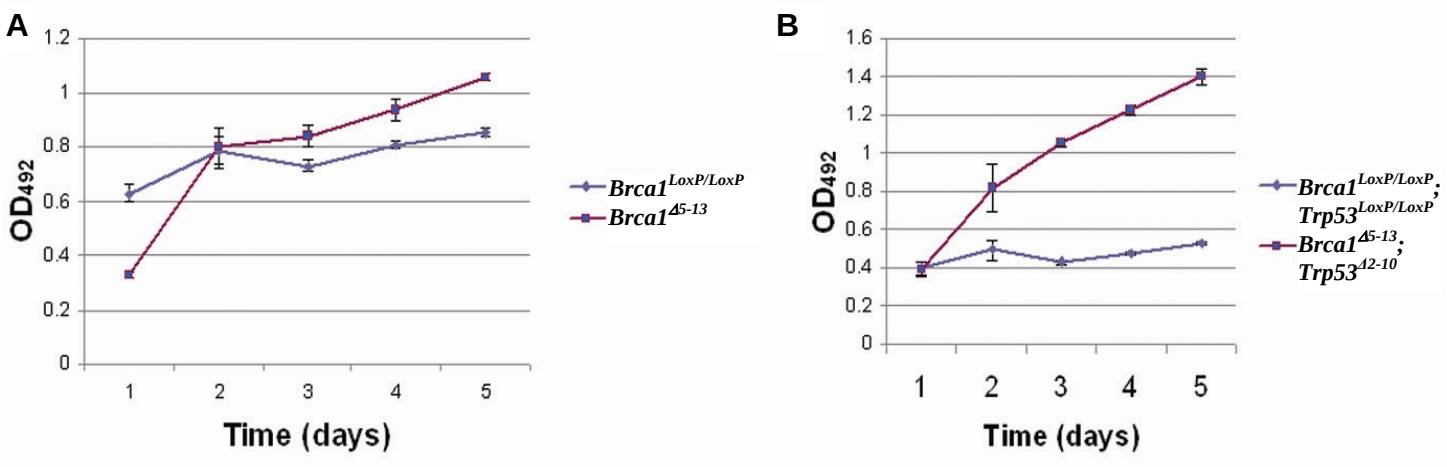

Figure 4. Effects of loss of *Brca1* or *Brca1* and *Trp53* inactivation on stromal cell proliferation. Stromal cells were seeded at 3,000 cells/well in a 96-well plate and proliferation evaluated over five day using the MTS assay. The graphs compare proliferation of A) $Brca1^{LoxP/LoxP}$ and $Brca1^{\Delta 5\text{-}13}$ and (B), $BRCA1^{LoxP/LoxP}$;$Trp53^{LoxP/LoxP}$ and $Brca1^{\Delta 5\text{-}13}$;$Trp53^{\Delta 2\text{-}10}$ ovarian stromal cells.

expression ($Brca1^{LoxP/LoxP}$ and $Brca1^{LoxP/LoxP}$;$Trp53^{LoxP/LoxP}$ cells, Fig. 2A and C). Col I staining showed punctate expression detectable in a subpopulation of stromal cells of all genotypes (Fig. 3). However, there appeared to be a decrease in either Col I-expressing cells or levels Col I protein expressed in $Brca1^{\Delta 5\text{-}13}$ and $Brca1^{\Delta 5\text{-}13}$;$Trp53^{\Delta 2\text{-}10}$ ovarian stromal cells compared to stromal cells with intact *Brca1* or *Brca1* and *Trp53*.

To determine if the increased thickness of the 3D stromal culture in $Brca11^{\Delta 5\text{-}13}$;$Trp53^{\Delta 2\text{-}10}$ stromal cells (Fig.2) was due to enhanced proliferation, cell viability was measured. Equal numbers of cells were plated on uncoated 96-well plates and total viability was assayed daily for five subsequent days by MTS Assay (Promega). A slight (<1.2-fold) increase in the total number of $Brca1^{\Delta 5\text{-}13}$ stromal cells was detected relative to control unexcised $Brca1^{LoxP/LoxP}$ cells (Fig.

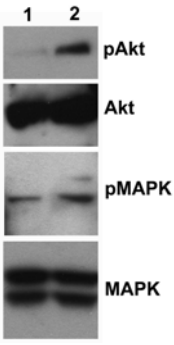

Figure 5. Akt and p42/44 MAPK are activated in $Brca1^{\Delta 5\text{-}13}$;$Trp53^{\Delta 2\text{-}10}$ ovarian stromal cells. Western blot detection of phosphorylated and total AKT, phosphorylated and total MAPK (p42/p44) in $Brca1^{LoxP/LoxP}$;$Trp53^{LoxP/LoxP}$ (lane 1) and $Brca1^{\Delta 5\text{-}13}$; $Trp53^{\Delta 2\text{-}10}$ (lane 2) ovarian stromal cells.

4A). By contrast, there was a significant increase in the number of viable *Brca1*$^{\Delta 5\text{-}13}$*;Trp53*$^{\Delta 2\text{-}10}$ ovarian stromal cells compared to unexcised *Brca1*$^{LoxP/LoxP}$*;Trp53*$^{LoxP/LoxP}$ control cells each day tested, reaching 2.7-fold higher levels by day 5 (Fig. 4B).

In addition to established roles in DNA damage repair, cell cycle checkpoint control, maintenance of genomic stability and transcription [13], a recent study showed that BRCA1 plays a role in controling Akt activation [14]. This study showed that BRCA1 physically interacts with phosphorylated AKT (pAKT) via the BRCA1-BRCT domain resulting in ubiquitination and degradation of the pAKT protein. Cells expressing mutant *BRCA1* or siRNAs targeting *BRCA1* showed increased levels and nuclear accumulation of pAkt protein [14]. In light of this observation, we hypothesized that activation of pAKT might contribute to the increase in proliferative capacity of ovarian stromal cells with conditionally inactivated *Brca1* and *Trp53*. We evaluated the expression of activated AKT and its downstream effector, MAPK, in *Brca1*$^{LoxP/LoxP}$*;Trp53*$^{LoxP/LoxP}$ and *Brca1*$^{\Delta 5\text{-}13}$*;Trp53*$^{\Delta 2\text{-}10}$ ovarian stromal cells by Western blot analysis and observed higher levels of activated pAKT and pMAPK in cells with conditional inactivation of both *Brca1* and *Trp53* (Fig. 5). Taken together, our results suggest that conditional inactivation of *Brca1* and *Trp53* in ovarian stromal cells confers a distinct proliferative advantage in these cells that may, in part, be due to AKT and MAPK activation.

To evaluate the paracrine effects stromal cells might exert on MOSE cells, we isolated MOSE cells from *Brca1*$^{LoxP/LoxP}$ mice and transduced them with recombinant adenovirus expressing either enhanced green fluorescent protein (*Ad5-CMV-eGFP*) or Cre-recombinase-eGFP (*Ad5-CMV-Cre-eGFP*). Transduction of *Brca1*$^{LoxP/LoxP}$ MOSE cells with the *Ad5-CMV-eGFP* fluorescent reporter resulted in efficient infection as evidenced by uniform expression of GFP in the transduced cells (Fig. 6A). To verify Cre-mediated excision of floxed sequences in *Ad5-CMV-Cre*-transduced cells, genomic DNA was isolated and subjected to PCR amplification as described [15]. Excision of floxed *Brca1* sequences resulted in deletion of exons 5-13 (Δ5-13) and was detected by amplification of the 594 nt excision product in *Ad5-CMV-Cre* transduced stromal (Fig. 6B) and MOSE cells (Fig. 6C). As expected, the 594 nt excision product was absent in stromal or MOSE cells transduced with *Ad5-CMV-eGFP* (Fig. 6B and C). To confirm the phenotypic effects of excision of floxed *Brca1* sequences, we performed indirect IF to detect the levels of BRCA1 and cytokeratin 19 (CK19) proteins. CK19 is an epithelial marker expressed in MOSE cells both *in vitro* and *in vivo*; therefore we evaluated its expression as a positive control in *Brca1*$^{LoxP/LoxP}$ MOSE cells transduced with either *Ad5-CMV-eGFP* or *Ad5-CMV-Cre-eGFP*. CK19 was uniformly expressed in both cultures confirming both the purity of the MOSE cell culture and the absence of non-specific effects of *Ad5-CMV-Cre* infection on protein expression (Fig. 7). *Brca1*$^{LoxP/LoxP}$ MOSE cells transduced with *Ad5-CMV-Cre-eGFP* exhibited significantly reduced BRCA1 protein levels compared to *Ad5-CMV-*

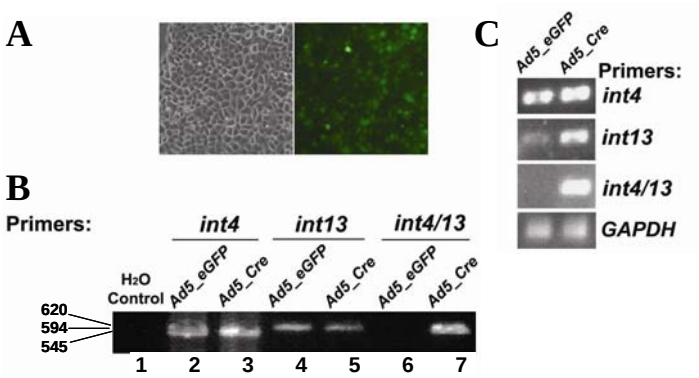

Figure 6. Adenoviral transduction of stromal and MOSE cells and Cre-mediated excision of LoxP flanked sequences. A) Brightfield (left) and fluorescent (right) images of *Brca1*$^{LoxP/LoxP}$ MOSE cells 72 h after transduction with *Ad5-CMV-eGFP*. B) PCR analyses of genomic DNA isolated from *Brca1*$^{LoxP/LoxP}$ stromal cells infected with *Ad5-CMV-eGFP or Ad5-CMV-Cre*. Amplification with primers specific for introns 4 (lanes 2 and 3) and 13 (lanes 4 and 5) resulted in detection of 545 nt and 620 nt PCR fragments, respectively, in cells infected with either *Ad5-CMV-eGFP* (lanes 2 and 4) *or Ad5-CMV-Cre* (lanes 3 and 5). Excision of LoxP flanked sequences in *Brca1*$^{LoxP/LoxP}$ stromal cells was detected by amplification of the 594 nt Δ5-13 product from genomic DNA using the 5'- int4 primer and the 3'-intron 13 primers. The Δ5-13 recombination product was detected in *Ad5-CMV-Cre* transduced (lane 7), but not *Ad5-CMV-eGFP* (lane 6) transduced stromal cells. C) Excision in *Brca1*$^{LoxP/LoxP}$ MOSE was detected by amplification of the Δ5-13 product in *Ad5-CMV-Cre* transduced (right), but not *Ad5-CMV-eGFP* (left) transduced MOSE cells.

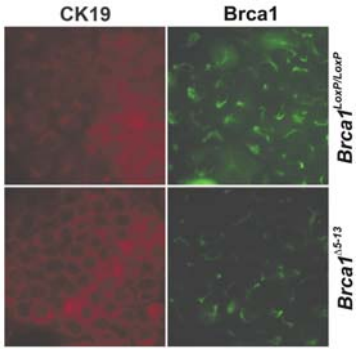

Figure 7. Brca1 and CK19 expression in MOSE cells after Cre-mediated excision of *Brca1*. Indirect IF staining of BRCA1 and cytokeratin 19, in *Brca1*$^{LoxP/LoxP}$ and *Brca1*$^{\Delta 5\text{-}13}$ MOSE cells.

eGFP transduced control cells (Fig. 7), confirming the effects of deletion of exons 5-13 in *Brca1*$^{\Delta 5\text{-}13}$ cells.

A previous study [15] showed that conditional inactivation of *Brca1* in *Brca1*$^{LoxP/LoxP}$ MOSE cells resulted in decreased proliferation. To investigate the effects of *Brca1* inactivation in the stroma on MOSE cell growth, MOSE cells were cultured on extracted 3D stromal cell-derived ECM in fresh medium, or on 3D stromal cell-derived ECM in the presence of conditioned culture medium isolated from stromal cells. The 3D ECM and conditioned medium (CM) were derived from stromal cells that were grown for 8 days in the presence of ascorbic acid to allow cells to secrete ECM and promote 3D growth. Conditioned medium was collected and stored at -80°C for later use. Stromal cells were extracted from the matrix by treatment with detergent and ammonium hydroxide [11], leaving a cell-free 3D ECM suitable for use as a growth substrate.

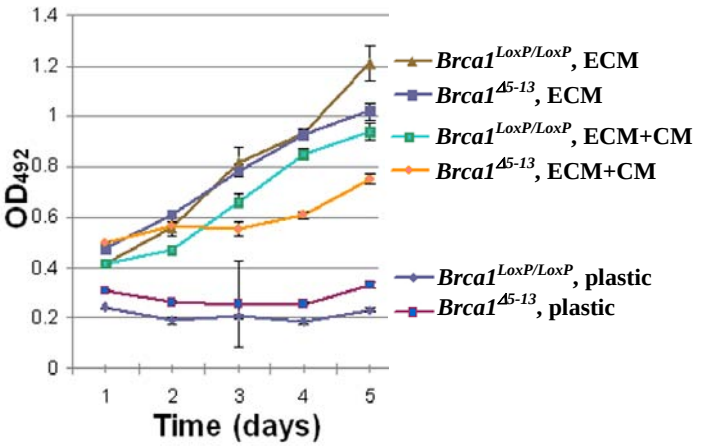

Figure 8. Effects of inactivation of *BRCA1* on MOSE proliferation. *Brca1*$^{LoxP/LoxP}$ and *Brca1*$^{\Delta 5\text{-}13}$ MOSE cells were seeded at 10,000 cells/well in a 96-well plate and MTS assays were performed to evaluate proliferation. Cells were cultured on: plastic (2D); 3D ECM from stromal cells of the same genotype; and 3D ECM and conditioned media (CM) from stromal cells of the same genotype.

We analyzed the growth of *Brca1*$^{\Delta 5\text{-}13}$ and *Brca1*$^{LoxP/LoxP}$ MOSE cells cultured on ECM derived from ovarian stromal cells of the same type (i.e., *Brca1*$^{\Delta 5\text{-}13}$ MOSE with *Brca1*$^{\Delta 5\text{-}13}$ ECM, and *Brca1*$^{LoxP/LoxP}$ MOSE with *Brca1*$^{LoxP/LoxP}$ ECM). The growth of both the *Brca1*$^{LoxP/LoxP}$ and *Brca1*$^{\Delta 5\text{-}13}$ MOSE cells on 3D stromal cell ECM was significantly increased compared to the same cells grown on uncoated plastic (Fig. 8). The growth of *Brca1*$^{LoxP/LoxP}$ and *Brca1*$^{\Delta 5\text{-}13}$ MOSE cells on 3D ECM was similar for the first four days, but by day five, growth of *Brca1*$^{LoxP/LoxP}$ MOSE cells significantly exceeded the *Brca1*$^{\Delta 5\text{-}13}$ MOSE cells (Fig.8). We then tested the effects of growth of *Brca1* inactivated and control MOSE cells on 3D ECM in the presence of CM collected from the same cells that produced the 3D ECM (i.e., *Brca1*$^{\Delta 5\text{-}13}$ MOSE with *Brca1*$^{\Delta 5\text{-}13}$ stromal ECM+CM, and *Brca1*$^{LoxP/LoxP}$ MOSE with *Brca1*$^{LoxP/LoxP}$ stromal ECM+CM). In the presence of both the 3D ECM and CM, the growth of *Brca1*$^{LoxP/LoxP}$ and *Brca1*$^{\Delta 5\text{-}13}$ MOSE cells was significantly increased over growth of the same cells grown on uncoated plastic. Consistent with the differences in growth of *Brca1*$^{LoxP/LoxP}$ and *Brca1*$^{\Delta 5\text{-}13}$ MOSE cells on ECM at day 5, the growth of *Brca1*$^{LoxP/LoxP}$ MOSE cells at days 3, 4, and 5 was significantly greater than the growth of *Brca1*$^{\Delta 5\text{-}13}$ MOSE cells (Fig. 8). Taken together, these results suggest stromal cells can produce ECM that support ovarian surface epithelial cell growth. However, loss of *Brca1* appears to result in diminished proliferative capacity MOSE cells.

Consistent with our results, Clarke-Knowles *et al.* [15], reported that conditional inactivation of *Brca1* in MOSE cells inhibited cell growth *in vitro*. However, the same study showed an increased number of neoplastic changes, including hyperplasia, invaginations and inclusion cysts in mice with Adenovirus-Cre-mediated inactivation of *Brca1* (*Brca1*$^{\Delta 5\text{-}13}$) compared to controls (*Brca1*$^{LoxP/LoxP}$) in mouse ovaries *in vivo*. These observations suggested the possibility that loss of functional *Brca1* might result in phenotypic changes such as enhanced invasive or migratory potential of MOSE cells that contributed to the described morphologic changes. To test this possibility, we compared the invasive capacity of *Brca1*$^{LoxP/LoxP}$ and *Brca1*$^{\Delta 5\text{-}13}$ MOSE cells in a modified Boyden chamber assay. Briefly, *Brca1*$^{LoxP/LoxP}$ and *Brca1*$^{\Delta 5\text{-}13}$ ovarian stromal

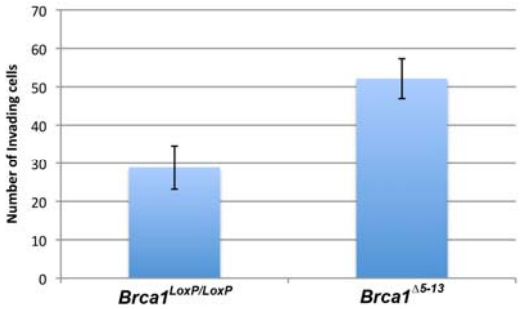

Figure 9. Invasive potential of *Brca1*$^{LoxP/LoxP}$ and *Brca1*$^{\Delta 5\text{-}13}$ MOSE cells. A modified Boyden chamber assay was performed using 3D ECM and conditioned media (CM) from *Brca1*$^{LoxP/LoxP}$ and *Brca1*$^{\Delta 5\text{-}13}$ stromal cells. *Brca1*$^{LoxP/LoxP}$ and *Brca1*$^{\Delta 5\text{-}13}$ MOSE cells were seeded on top of the ECM in duplicate inserts and allowed to invade for 96 h. Invasive cells were fixed, stained for DAPI, and quantified by counting 5 fields; $P < 0.05$.

cells were cultured in the top chamber of the Boyden chamber for 8 days to allow 3D growth and deposition of ECM. The stromal cells were then extracted as described above. *Brca1*$^{LoxP/LoxP}$ or *Brca1*$^{\Delta 5\text{-}13}$ MOSE cells were then seeded on the extracted *Brca1*$^{LoxP/LoxP}$ and *Brca1*$^{\Delta 5\text{-}13}$ stromal ECM in the top chamber and allowed to invade toward ovarian stromal cells CM in the bottom chamber. Interestingly, we observed that *Brca1*$^{\Delta 5\text{-}13}$ MOSE cells showed significantly increased invasive potential (1.8 fold, $p < 0.05$) relative to control *Brca1*$^{LoxP/LoxP}$ MOSE cells (Fig. 9). These results suggest that while loss of *Brca1* inhibits MOSE cell proliferation, it increases the capacity of these cells to invade through stromal extracellular matrix.

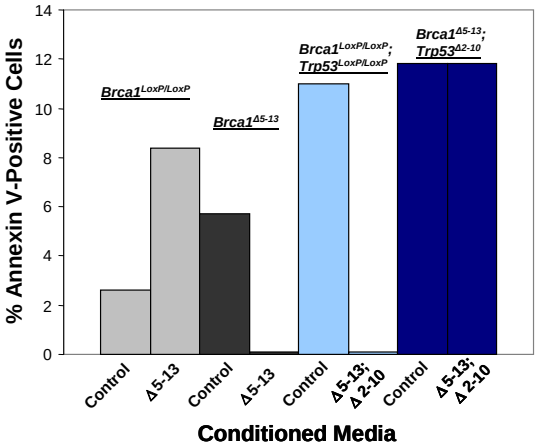

Figure 10. Secreted factors from 3D stromal cells influences apoptosis in MOSE cells. MOSE cells were grown on standard (2D) cell culture plastic in the absence (control) or presence or of conditioned medium (CM) from 3D stromal cell cultures of the same genotype. The genotypes of MOSE cells are indicated above the bars. The presence of CM from either control (Con), *Brca1*$^{\Delta 5\text{-}13}$ (*Δ5-13*), or *Brca1*$^{\Delta 5\text{-}13}$*;Trp53* $^{\Delta 2\text{-}10}$ (*Δ5-13;Δ2-10*) stromal cultures is indicated on the X-axis. Apoptosis was assayed using the Guava Nexin system in which cells are labeled with Annexin V. Data are presented as the percentage of annexin V-positive cells.

Next, we tested whether paracrine factors secreted by ovarian stromal cells influence apoptosis in MOSE cells. MOSE cells were grown on cell culture plastic (2D) in the absence or presence of conditioned medium (CM) isolated from control (*Brca1*$^{LoxP/LoxP}$) or mutant (*Brca1*$^{\Delta 5\text{-}13}$) 3D stromal cell cultures. Growth of *Brca1*$^{LoxP/LoxP}$ MOSE cells in the presence of CM from mutant stromal cells resulted in a dramatic increase (~3.2-fold) in apoptosis compared *Brca1*$^{LoxP/LoxP}$ MOSE cells in control CM (Fig. 10, light grey bars). In contrast, culture of *Brca1*$^{\Delta 5\text{-}13}$ MOSE in the presence of CM from mutant stromal cells resulted in a dramatic reduction in the number of apoptotic cells compared to growth in the presence of control CM (Fig. 10, dark grey bars). For *Brca1*$^{LoxP/LoxP}$*;Trp53*$^{LoxP/LoxP}$ MOSE cells, the number of apoptotic cells was also dramatically lower when cultured with mutant CM compared to control CM (Fig. 10, light blue bars). Apoptosis in *Brca1*$^{\Delta 5\text{-}13}$*;Trp53*$^{\Delta 2\text{-}10}$ MOSE cells was equivalent in the presence of control or mutant CM (Fig. 10, dark blue bars). Collectively, these results suggest that paracrine factors secreted by stromal cells can affect programmed cell death in epithelial cells, and that these effects differ depending upon the genetic background of the stromal and epithelial cells. For example, factors secreted from *Brca1*$^{\Delta 5\text{-}13}$ stromal cells resulted in increased apoptosis in *Brca1*$^{LoxP/LoxP}$ MOSE cells, but decreased apoptosis in *Brca1*$^{\Delta 5\text{-}13}$ and *Brca1*$^{\Delta 5\text{-}13}$*;Trp53*$^{\Delta 2\text{-}10}$ MOSE cells.

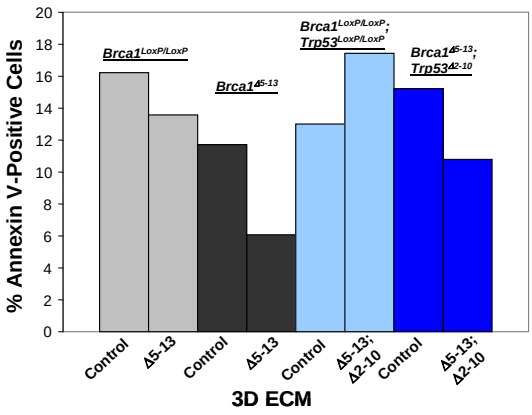

Figure 11. Growth of MOSE cells on 3D ECM alters apoptosis. MOSE were cultured in 3D ECM isolated from control , *Brca1*$^{\Delta 5\text{-}13}$ (*Δ5-13*), or *Brca1*$^{\Delta 5\text{-}13}$*;Trp53*$^{\Delta 2\text{-}10}$ (*Δ5-13;Δ2-10*) stromal cultures as indicated on the X-axis. The genotypes of MOSE cells are indicated above the bars. Apoptosis was assayed using the Guava Nexin system in which cells are labeled with Annexin V. Data are presented as the percentage of annexin V-positive cells.

Similar experiments were performed to evaluate the effects of interactions between epithelial cells and the 3D stromal ECM on apoptosis. Control and mutant MOSE cells were grown on ECM derived from control or mutant stromal cells. *Brca1*$^{LoxP/LoxP}$ MOSE cultured on 3D *Brca1*$^{\Delta 5\text{-}13}$ stromal cell ECM exhibited a modest decrease in apoptosis compared cells grown on control 3D ECM (Fig. 11, light grey bars). A dramatic 48% decrease in apoptosis was observed in *Brca1*$^{\Delta 5\text{-}13}$ MOSE cells grown on mutant *Brca1*$^{\Delta 5\text{-}13}$ 3D ECM compared to control ECM (Fig. 11, dark grey bars). A slight increase (1.3-fold) in apoptosis was observed in *Brca1*$^{LoxP/LoxP}$*;Trp53*$^{LoxP/LoxP}$ MOSE cells cultured on mutant *Brca1*$^{\Delta 5\text{-}13}$*;Trp53* $^{\Delta 2\text{-}10}$ ECM compared to control ECM (Fig. 11, light blue bars). However, apoptosis was significantly decreased (29%) in mutant *Brca1*$^{\Delta 5\text{-}13}$*;Trp53* $^{\Delta 2\text{-}10}$ MOSE cells cultured on mutant *Brca1*$^{\Delta 5\text{-}13}$*;Trp53* $^{\Delta 2\text{-}10}$ ECM compared to

control ECM (Fig. 11, dark blue bars). Similar to the effects of conditioned medium, these observations suggest that interactions between epithelial cells and 3D matrices can either positively or negatively regulate apoptosis depending upon the genetic background of the MOSE cells and the stromal cells from which the matrix was derived. Overall, substantially less programmed cell death is observed in mutant MOSE cells cultured on mutant ECM compared to control ECM.

We extended our analysis of the growth of MOSE cells on 3D ECM by comparing the proliferation of control (*Brca1*$^{LoxP/LoxP}$ and *Brca1*$^{LoxP/LoxP}$*;Trp53*$^{LoxP/LoxP}$) and mutant (*Brca1*$^{\Delta 5\text{-}13}$ cells *Brca1*$^{\Delta 5\text{-}13}$*;Trp53* $^{\Delta 2\text{-}10}$) MOSE cells on control and mutant 3D stromal cell ECM. MOSE cells were cultured on 2D plastic or 3D ECM over a period of 5-7 days and cell viability was analyzed every two days to examine the growth rate. Regardless of growth substrate, *Brca1*$^{LoxP/LoxP}$ MOSE cells exhibited a growth advantage over *Brca1*$^{\Delta 5\text{-}13}$ MOSE cells (Fig. 12A, B and C). This is consistent with our own previous experiments (Fig. 8) and a previous study [15] showing that inactivation of *Brca1* in MOSE cells resulted in decreased proliferation *in vitro*. Our results further extend this observation by showing that proliferation of either *Brca1*$^{LoxP/LoxP}$ or *Brca1*$^{\Delta 5\text{-}13}$ MOSE cells cultured on 3D ECM isolated from stromal cells with inactivated *Brca1* is diminished compared to cells grown on control ECM isolated from *Brca1*$^{LoxP/LoxP}$ stromal cells (Figs. 12B & C). This suggests that loss of *Brca1* in the tumor microenvironment has a dominant growth inhibitory effect on the growth of MOSE cells.

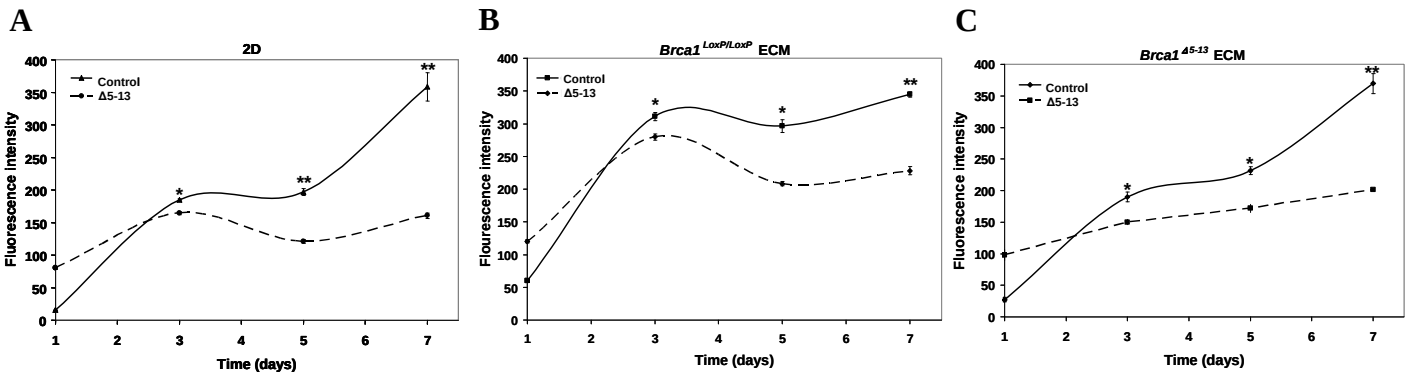

Figure 12. Growth rates of *Brca1*$^{LoxP/LoxP}$ and *Brca1*$^{\Delta 5\text{-}13}$ MOSE on a 2D plastic and on 3D ECM. The growth of MOSE cells cultured on plastic or 3D ECM was evaluated over a period of 7 days. Graphs depicting growth of MOSE on different substrates are shown (A-C). A) *Brca1*$^{LoxP/LoxP}$ and *Brca1*$^{\Delta 5\text{-}13}$ MOSE cells grown on a 2D (plastic) substrate; B) *Brca1*$^{LoxP/LoxP}$ and *Brca1*$^{\Delta 5\text{-}13}$ MOSE cells grown on control *Brca1*$^{LoxP/LoxP}$ stromal 3D ECM; C) *Brca1*$^{LoxP/LoxP}$ and *Brca1*$^{\Delta 5\text{-}13}$ MOSE cells grown on mutant *Brca1*$^{\Delta 5\text{-}13}$ stromal 3D ECM. Cell viability was measured in triplicate for each sample using the Cell Titer Blue assay and presented as fluorescence intensity. Data are presented as means ± SE. Statistically significant differences in cell viability at days 3, 5, and 7 were determined using a Student's *t*-test (*, $P < 0.05$; **, $P < 0.001$).

In contrast to inactivation of *Brca1* alone, conditional inactivation of both *Brca1* and *Trp53* results in an increased proliferative capacity of MOSE cells (Figure 13A, B and C). The increased growth rate of *Brca1*$^{\Delta 5\text{-}13}$*;Trp53*$^{\Delta 2\text{-}10}$ MOSE cells compared to *Brca1*$^{LoxP/LoxP}$*;Trp53*$^{LoxP/LoxP}$ MOSE cells is observed in cells grown on 2D plastic (Fig 13A), but is even more pronounced in cells grown on 3D stromal ECM regardless of the *Brca1* and *Trp53* status of the stromal cells (compare Figs. 13B & 13C to 13A). These findings indicate that in contrast to loss of *Brca1*, inactivation of *Trp53* confers a substantial proliferative advantage in MOSE cells that is enhanced by the 3D ECM microenvironment.

Our results confirm that interactions between ovarian surface epithelial cells and a 3D stromal cell-derived ECM-derived microenvironment can dramatically affect the proliferation of MOSE cells *in vitro*. They further demonstrate that a stromal cell-derived 3D ECM in which *Brca1* has been inactivated can mediate growth suppressive signaling pathways while a stromal cell-derived 3D ECM in which *Trp53* has been inactivated can mediate growth stimulatory signals. A possible explanation for the observed decrease in growth in *Brca1* mutant MOSE cells may be due to activation of p53 [15] and its downstream effector, p21, since deletion of p53 and/or p21 partially rescues the lethality observed in *Brca1*-null embryos [9, 16-18]. Previous studies reveal that *Brca1* inactivation results in growth suppression by activation of senescence pathways that are p21-dependent

[9, 19]. Also, loss of a tumor suppressor such as *Brca1* can induce a DNA damage response that activates pathways that includes ATM, Chk1, Chk2, p21, and Gadd45 to prevent cell division [13]. In support of this, one study demonstrated that, in *Brca1* deficient cells, Chk2 is phosphorylated, resulting in the accumulation and activation p53 [17]. Since we observed a decrease in apoptosis when *Brca1*$^{\Delta 5\text{-}13}$ MOSE cells were cultured with CM or on 3D ECM derived from *Brca1*$^{\Delta 5\text{-}13}$ stromal cells, it is possible that the observed diminution in growth is due to activation of one or more mediators of the DNA damage response pathways. This suggests that loss of

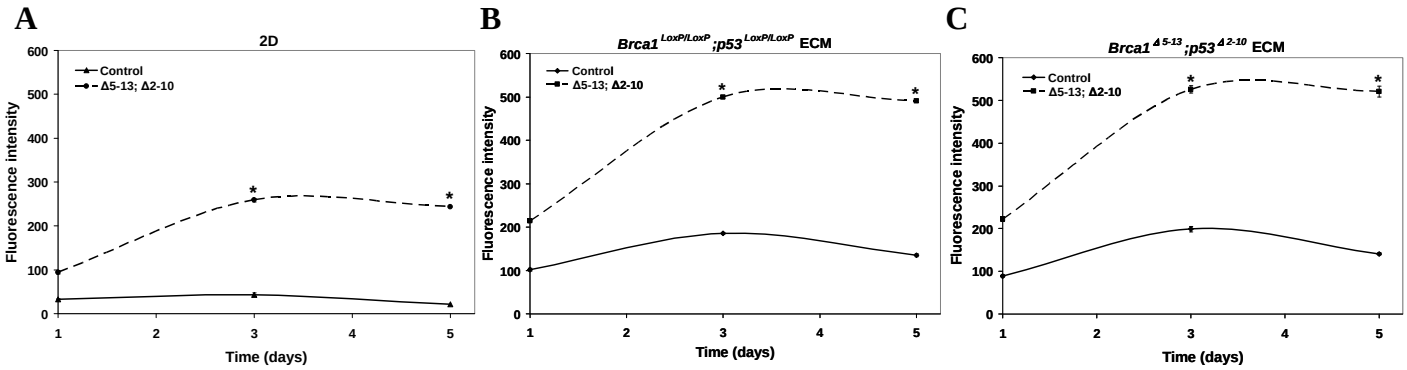

Figure 13. Growth rates of *Brca1*$^{LoxP/LoxP}$;*Trp53*$^{LoxP/LoxP}$ and *Brca1*$^{\Delta 5\text{-}13}$;*Trp53*$^{\Delta 2\text{-}10}$ on a 2D surface and on 3D ECM. The growth of MOSE cells cultured on plastic or 3D ECM was evaluated over a period of 5 days. Graphs depicting growth of MOSE cells on different substrates are shown (A-C). A) *Brca1*$^{LoxP/LoxP}$;*Trp53*$^{LoxP/LoxP}$ (control) and *Brca1*$^{\Delta 5\text{-}13}$;*Trp53*$^{\Delta 2\text{-}10}$ (*Δ5-13;Δ2-10*) MOSE cells grown on 2D; B) *Brca1*$^{LoxP/LoxP}$;*Trp53*$^{LoxP/LoxP}$ (control) and *Brca1*$^{\Delta 5\text{-}13}$;*Trp53*$^{\Delta 2\text{-}10}$ (*Δ5-13;Δ2-10*) MOSE cells grown on control *Brca1*$^{LoxP/LoxP}$;*Trp53*$^{LoxP/LoxP}$ stromal 3D ECM, and C) *Brca1*$^{LoxP/LoxP}$;*Trp53*$^{LoxP/LoxP}$ (control) and *Brca1*$^{\Delta 5\text{-}13}$;*Trp53*$^{\Delta 2\text{-}10}$ (*Δ5-13;Δ2-10*) MOSE cells grown on mutant *Brca1*$^{\Delta 5\text{-}13}$;*Trp53*$^{\Delta 2\text{-}10}$ stromal 3D ECM. Cell viability was measured in triplicate for each sample using the Cell Titer Blue assay and presented as fluorescent intensity. Data are presented as means ± SE. Statistically significant differences in cell viability at days 3 and 5 were determined using a Student's *t*-test (*$P < 0.001$).

Brca1 may favor activation of senescence pathways rather than apoptotic pathways in MOSE cells. Subsequent loss of *Trp53* may release cells from the growth inhibitory effects of *Brca1* inactivation and promote tumorigenesis.

Key Research Accomplishments:

- Developed a 3D *in vitro* model system
- Characterized FN and type I collagen in 3D ovarian stromal cell cultures
- Analyzed proliferation in stromal cells with conditional inactivation of *Brca1* alone or in combination with *Trp53*
- Optimized efficient adenovirus transduction of MOSE cells for Cre-mediated excision of *Brca1* or *Brca1* and *Trp53*
- Analyzed proliferative capacity of *Brca1*$^{LoxP/LoxP}$ and *Brca1*$^{\Delta 5\text{-}13}$ MOSE cells grown on 3D ECM isolated from ovarian stromal cells and on 3D ECM and conditioned media from isolated from ovarian stromal cells
- Characterized the invasive potential of *Brca1*$^{LoxP/LoxP}$ and *Brca1*$^{\Delta 5\text{-}13}$ MOSE cells through ovarian stromal cell ECM
- Analyzed the growth of *Brca1*$^{LoxP/LoxP}$ and *Brca1*$^{\Delta 5\text{-}13}$ MOSE cells cultured within a 3D ECM isolated from stromal cells with functional or inactivated *Brca1* or *Brca1* and *Trp53*
- Evaluated the effects of *Brca1* or *Brca1* and *Trp53* excision on apoptosis in MOSE cells cultured in the presence of conditioned culture medium isolated from stromal cells with functional or inactivated *Brca1* or *Brca1* and *Trp53*

- Evaluated the effects of *Brca1* or *Brca1* and *Trp53* excision on apoptosis of 3D matrices isolated from stromal cells with functional or inactivated *Brca1* or *Brca1* and *Trp53*

Reportable Outcomes:

- Inactivation of *Brca1* and *53* results in a dramatic increase in proliferation and AKT activation in ovarian stromal cells.
- MOSE cells cultured on 3D stromal cell ECM or 3D stromal ECM and conditioned medium exhibit increased proliferation compared to cells grown on plastic.
- Inactivation of *Brca1* results in diminished capacity of ovarian stromal cell ECM and CM to support MOSE proliferation.
- Inactivation of *Brca1* in MOSE cells results in a significant increase in invasive capacity.
- Factors present in conditioned culture medium from 3D stromal cultures can alter apoptosis in ovarian surface epithelial cells depending on *Brca1* and *Trp53* status.
    - Apoptosis is elevated in $Brca1^{LoxP/LoxP}$ MOSE cells cultured with CM from *Brca1* mutant stromal cells relative to control CM.
    - Apoptosis is decreased in *Brca1* mutant MOSE cells cultured with CM from *Brca1* mutant stromal cells relative to control CM.
    - Apoptosis is decreased in $Brca1^{LoxP/LoxP}$;Tr$p53^{LoxP/LoxP}$ MOSE cells cultured with CM from stromal cells mutant for both *Brca1* and *Trp53* compared to control CM.
- Stromal cell-derived ECM can influence apoptosis in MOSE cells.
    - Apoptosis is decreased in MOSE cells mutant for *Brca1* or *Brca1* and *Trp53* cultured on ECM isolated from mutant stromal cells compared to control ECM.
- The *Brca1* mutant 3D ECM has a dominant growth suppressive effect on both $Brca1^{LoxP/LoxP}$ and inactivated *Brca1* MOSE cells.
- Inactivation of *Trp53* confers a significant proliferative advantage in MOSE cells grown in 2D and on 3D ECM.

Conclusions:

Our data support the hypothesis that the surrounding ovarian stroma exerts significant effects on the growth and physiology of ovarian surface epithelium. Both the 3D ECM and factors secreted by the stromal cells can alter the proliferation and invasive potential of MOSE cells. We have begun analyzing the signaling pathways which may play a critical role in regulating the phenotypic changes that occur in cells which are deficient for *Brca1* or *Brca1* and *Trp53*. Using this 3D *in vitro* model system will allow us to address basic questions concerning the pathological development of ovarian cancer in a setting which is more representative of the *in vivo* environment.

We are in the process of independent validation of key experiments prior to submission of a manuscript describing our results (Do, T.V., Bickel, L. and Connolly, D.C. Conditional inactivation of *Brca1* or *Brca1* and *Trp53* in the Ovarian Stroma Influences Growth and Transformation Potential of the Ovarian Surface Epithelium. In preparation, planned submission winter 2010)

Literature Cited:

1. Brose, M.S., et al., *Cancer risk estimates for BRCA1 mutation carriers identified in a risk evaluation*

program. J Natl Cancer Inst, 2002. **94**(18): p. 1365-72.
2. Buller, R.E., et al., *The p53 mutational spectrum associated with BRCA1 mutant ovarian cancer.* Clin Cancer Res, 2001. **7**(4): p. 831-8.
3. Ramus, S.J., et al., *Increased frequency of TP53 mutations in BRCA1 and BRCA2 ovarian tumours.* Genes Chromosomes Cancer, 1999. **25**(2): p. 91-6.
4. Rhei, E., et al., *Molecular genetic characterization of BRCA1- and BRCA2-linked hereditary ovarian cancers.* Cancer Res, 1998. **58**(15): p. 3193-6.
5. Schorge, J.O., et al., *BRCA1-related papillary serous carcinoma of the peritoneum has a unique molecular pathogenesis.* Cancer Res, 2000. **60**(5): p. 1361-4.
6. Chodankar, R., et al., *Cell-nonautonomous induction of ovarian and uterine serous cystadenomas in mice lacking a functional Brca1 in ovarian granulosa cells.* Curr Biol, 2005. **15**(6): p. 561-5.
7. Hill, R., et al., *Selective evolution of stromal mesenchyme with p53 loss in response to epithelial tumorigenesis.* Cell, 2005. **123**(6): p. 1001-11.
8. Patocs, A., et al., *Breast-cancer stromal cells with TP53 mutations and nodal metastases.* N Engl J Med, 2007. **357**(25): p. 2543-51.
9. Weber, F., et al., *Total-genome analysis of BRCA1/2-related invasive carcinomas of the breast identifies tumor stroma as potential landscaper for neoplastic initiation.* Am J Hum Genet, 2006. **78**(6): p. 961-72.
10. Coppe, J.P., et al., *Senescence-associated secretory phenotypes reveal cell-nonautonomous functions of oncogenic RAS and the p53 tumor suppressor.* PLoS Biol, 2008. **6**(12): p. 2853-68.
11. Beacham, D.A. and E. Cukierman, *Stromagenesis: the changing face of fibroblastic microenvironments during tumor progression.* Semin Cancer Biol, 2005. **15**(5): p. 329-41.
12. Cukierman, E., *Cell Migration: Developmental Methods and Protocols*. Methods in Molecular Biology, ed. J.-L. Guan. Vol. 294. 2005, Totowa, NJ: Humana Press Inc. 79-93.
13. Narod, S.A. and W.D. Foulkes, *BRCA1 and BRCA2: 1994 and beyond.* Nat Rev Cancer, 2004. **4**(9): p. 665-76.
14. Xiang, T., et al., *Negative Regulation of AKT Activation by BRCA1.* Cancer Res, 2008. **68**(24): p. 10040-4.
15. Clark-Knowles, K.V., et al., *Conditional inactivation of Brca1 in the mouse ovarian surface epithelium results in an increase in preneoplastic changes.* Exp Cell Res, 2007. **313**(1): p. 133-45.
16. Xu, B., S. Kim, and M.B. Kastan, *Involvement of Brca1 in S-phase and G(2)-phase checkpoints after ionizing irradiation.* Mol Cell Biol, 2001. **21**(10): p. 3445-50.
17. McPherson, J.P., et al., *Collaboration of Brca1 and Chk2 in tumorigenesis.* Genes Dev, 2004. **18**(10): p. 1144-53.
18. Ludwig, T., et al., *Targeted mutations of breast cancer susceptibility gene homologs in mice: lethal phenotypes of Brca1, Brca2, Brca1/Brca2, Brca1/p53, and Brca2/p53 nullizygous embryos.* Genes Dev, 1997. **11**(10): p. 1226-41.
19. Brodie, S.G., et al., *Multiple genetic changes are associated with mammary tumorigenesis in Brca1 conditional knockout mice.* Oncogene, 2001. **20**(51): p. 7514-23.

Bibliography of Publications:

None

List of Personnel:

Denise C. Connolly, Ph.D. – Principal Investigator
Thuy-Vy Do, Ph.D. – Research Associate